

Semiconductor Electrodes

VIII. Digital Simulation of Open-Circuit Photopotentials

Daniel Laser and Allen J. Bard*

Department of Chemistry, The University of Texas at Austin, Austin, Texas 78712

ABSTRACT

A simulation technique is described for the calculation of semiconductor electrode properties at steady state, *e.g.*, at equilibrium in the dark or under constant illumination. Integration of the continuity equation with respect to distance at the steady state yields a relation between the light flux and free carriers, which can be used in a recursion relation to determine the free carrier concentrations and the electric field within the space charge region of the semiconductor electrode. The technique is used to calculate the Boltzmann distribution within the semiconductor electrode and to determine the photopotential in the absence of faradaic current and surface states.

In a previous paper in this series (1) we described a digital simulation method for semiconductor electrodes and the formation of the space charge region in a semiconductor electrode upon charge injection. The main motivation for these simulations has been the recent interest in semiconductor electrodes and their application to photoelectrochemical cells and devices (2). One characteristic of interest is the change in surface potential of a semiconductor/electrolyte interface under illumination, the photopotential. Although theoretical treatments of the photopotential have been given (3, 4), and its magnitude related to the semiconductor properties, surface potential, and light intensity, these treatments usually involve restrictive conditions, (*e.g.*, total light absorption in the space charge region, minority carrier diffusion length much larger than the size of the space charge region). We describe here the digital simulation of the steady-state photopotential which arises upon illumination of a semiconductor electrode previously brought to a given potential and now held at open circuit. Charge transfer reactions, *e.g.*, open-circuit corrosion, are assumed not to occur during this illumination.

Physical Model

The general equation for the processes within a semiconductor electrode under illumination can be obtained by considering the creation of electron/hole pairs by light absorption, their mass transfer by diffusion and migration, and their recombination. Thus the change in concentration of holes, p , at a given location in the semiconductor is given (in one-dimensional form) by

$$\partial p / \partial t = \partial j_p(x) / \partial x + I_0 a e^{-ax} - R(x) \quad [1]$$

where I_0 is the intensity of light incident on the semiconductor/electrolyte interface (taken as $x = 0$), a is the coefficient of light absorption of the semiconductor, $j_p(x)$ is the total flux of holes at x , and $R(x)$ the rate of electron/hole recombination. We are concerned here with the steady-state photopotential. Thus with $\partial p / \partial t = 0$, integration of Eq. [1] yields

$$j_p(x) - j_p(0) = \int_0^x R(x) dx - I_0(1 - e^{-ax}) \quad [2]$$

where $j_p(0)$ is the flux of holes crossing the interface, or the hole contribution to the faradaic current density, i_p . Thus

$$j_p(x) = i_p/e - I_0(1 - e^{-ax}) + \int_0^x R(x) dx \quad [3]$$

A similar expression can be written for electrons

$$j_n(x) = i_n/e + I_0(1 - e^{-ax}) - \int_0^x R(x) dx \quad [4]$$

where $j_n(x)$ and i_n are the electron flux and the electron contribution to the faradaic current density, respectively. The light flux and electron flux are taken as positive going into the semiconductor from the solution and the hole flux is positive going out of the semiconductor to the solution. (A representation of the fluxes is shown in Fig. 1.) Equations [3] and [4] hold at all x , both within and outside of the space charge region. The net current density at any x , i , is given by Eq. [5]

$$j_p(x) + j_n(x) = (i_p + i_n)/e = i \quad [5]$$

i.e., at steady state a current (which may be zero) flows through the semiconductor phase. Equations [3] and [4] are employed in a digital or finite difference form in the simulation. The procedure follows the usual digital simulation approach (5). The semiconductor region of interest is divided into space elements of width Δx which are assigned an index K , from $K = 1$ (surface element) to $K = KMAX$ (Fig. 1). The carrier concentration within each element is assumed constant and represents the average value of p_K and n_K for holes and electrons, respectively, at that location. The electric field at the left boundary (the solution side) of element K , *i.e.*, between it and element $K - 1$, is denoted E_K and the carrier concentration at this

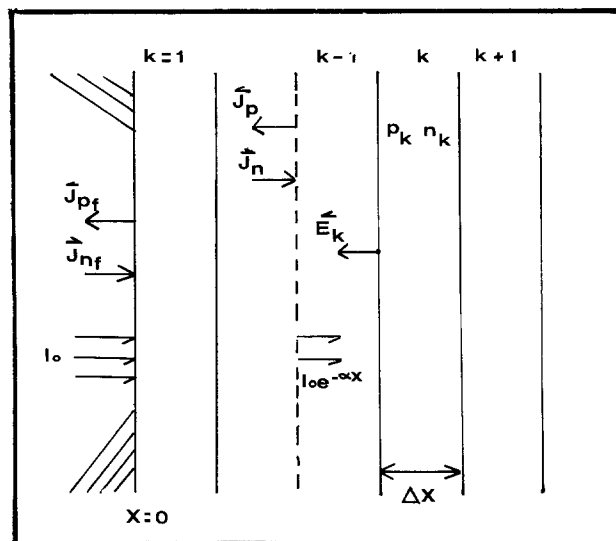


Fig. 1. Digital representation of the semiconductor phase and flux notation.

* Electrochemical Society Active Member.
Key words: semiconductors, digital simulation, photopotentials, photoeffects.

Table I. Comparison of differential and finite difference notation

| Quantity | Differential notation | Finite difference notation |
|---------------------------------------------------------------------------------|----------------------------------------------|---------------------------------------------|
| Distance, x | | $(K - \frac{1}{2})\Delta x$ |
| Migration flux of holes, $j_{p,m}$ | $D_p \frac{\partial p}{\partial x}$ | $\frac{1}{2} U_p E_K (p_K + p_{K-1})$ |
| Diffusional flux of holes, $j_{p,d}$ | $(1/\epsilon_0 \epsilon_r) \int_0^x Q(x) dx$ | $D_p (p_{K-1} - p_K)/\Delta x$ |
| Electric field, E | | $\sum_{K=0}^{KMAX} (p_K - n_K + N_D - N_A)$ |
| Recombination rate, $R(x)$ (e.g., for excess holes in an n-type semiconductor)* | $k_r n(x) (p(x) - p^{eq})$ | $(n_K/\tau_p n_b) (p_K - p_K^{eq})$ |

* $\partial p(x)/\partial t = k_r n(x)p(x) - k_t$, where k_r is the recombination rate constant given by $1/\tau_p n_b$ and k_t is the formation constant, given by $k_r n^{eq} p^{eq}$ (the superscript eq denotes the equilibrium concentrations in the n-type semiconductor). The equation in the table results when $n^{eq} \approx n(x)$.

boundary is taken as the average of that of the two adjacent elements [e.g., $\frac{1}{2}(p_K + p_{K-1})$]. A comparison of the differential and finite difference notation used in the simulation for expressing fluxes and other quantities of interest is given in Table I.

Initial conditions. The Boltzmann distribution.—The distribution of the carriers and the electric field in the semiconductor biased to a known potential (thus containing a known excess charge) and at equilibrium in the dark serves as the initial state preceding calculation of the photopotential. This equilibrium distribution is of fundamental importance in understanding and predicting the electrochemical behavior of semiconductor electrodes and is assumed to be essentially obeyed even in nonequilibrium situations (4-6). This distribution is usually obtained by using Fermi statistics for the occupancy of allowed energy states for which $\exp[(E - E_F)/kT] \ll 1$ and which physically means that at low occupancy, spin requirements may be relaxed. In addition, the Poisson equation must be solved using charge density terms which are based on the equilibrium distribution of carriers as functions of a coordinate which is not yet explicitly known (7). In general, a closed-form explicit relation between the potential and its gradient cannot be obtained for a doped semiconductor (8). At equilibrium in the dark, there is no faradaic current and no excess free carriers to give nonequilibrium recombination effects. Thus Eq. [3] and [4] yield

$$j_p(x) = j_n(x) = 0 \quad (\text{for all } x) \quad [6]$$

and at the boundary of each element, the migrational flux is compensated by the diffusional one for both electrons and holes. Equating these fluxes using the digital-form equations in Table I and rearranging, we obtain

$$p_K = \frac{(D_p/\Delta x) - 0.5U_p E_K}{(D_p/\Delta x) + 0.5U_p E_K} p_{K-1} \quad [7]$$

$$n_K = \frac{(D_n/\Delta x) + 0.5U_n E_K}{(D_n/\Delta x) - 0.5U_n E_K} n_{K-1} \quad [8]$$

Equations [7] and [8] are used as recursion relations in an iterative computation beginning with the second element ($K = 2$). For the first element (the semiconductor surface) the boundary conditions are (9)

$$p_1 = p^0 \exp(eV_s/kT) \quad [9a]$$

$$n_1 = n^0 \exp(-eV_s/kT) \quad [9b]$$

where V_s is the applied surface potential governing the distribution. The U and D values in Eq. [7] and [8] are related to each other via the Einstein relation

$$U(\text{cm}^2 \text{sec}^{-1} \text{V}^{-1}) = D/kT = 39D(\text{cm}^2 \text{sec}^{-1}) \quad [10]$$

at room temperature. A recursion relation for the electric field, E_K , which takes account of the semiconductor properties (dielectric constant, doping level) is obtained from Gauss' law

$$E_K = E_{K+1} + (e\Delta x/\epsilon_0 \epsilon_r) (p_K - n_K + N_D - N_A) \quad [11]$$

The boundary condition used with this relation is that in the bulk semiconductor ($K \cong KMAX$), $E_K = 0$. The simulation proceeds by using the applied potential in the boundary condition, Eq. [9], and then calculating n_K and p_K ($K = 1$ to $KMAX$) assuming any arbitrary initial distribution (usually taken as a uniform one, i.e., a flatband condition). The E_K values are then calculated, using Eq. [11]. Alternate calculations of n_K , p_K , and E_K are continued until the three arrays are constant with respect to further iterations. The resulting values, besides satisfying Eq. [7]-[11], also show the following features: (i) a numerical integration over the electric field from the bulk to the surface of the semiconductor yields the surface potential governing the distribution (which enters into the simulation only in assigning p_1 and n_1), thus demonstrating self-consistency in V_s ; (ii) the product $p_K n_K$ is constant and equal to n_i^2 (e.g., for Ge $n_i^2 = 6.25 \times 10^{16} \text{cm}^{-6}$ at room temperature) for all K .

A problem arises in the selection of $KMAX$. If this value is too large, the simulation does not converge to a constant solution. Since the value of $KMAX$, representing the thickness of the space charge region, is not known in advance, an arbitrary value which will yield a solution is chosen and when a convergent solution is obtained, $KMAX$ is increased. The calculation terminates with the highest value of $KMAX$ which still gives a constant solution. Inspection of the result shows that only the very diffuse part of the space charge region, which contributes insignificantly (<1%) to the electrical state (fields, potentials) of the semiconductor cannot be displayed.

Note that in contrast to our previous simulation of space charge region formation in a semiconductor following charge injection which portrayed the time dependence of the fields and concentration profiles (1), the method employed here derives only the equilibrium properties at a given potential. The concept of time is omitted and the intermediate results have no physical meaning. Typical equilibrium concentration profiles of the mobile carriers in intrinsic and n-type Ge at several surface potentials obtained by the simulation are shown in Fig. 2-4. Figures 2 and 3 illustrate the final equilibrium situation under the same conditions as the relaxation results given previously (1). A comparison of the surface potential and space charge layer thickness (or Debye length) for a highly doped semiconductor obtained by the approximate "depletion layer" treatment, which underlies the Schottky-Mott plot (10), and our calculation is given in Table II. Note that the approximation becomes less applicable at low potentials when the concentration of the existing carriers in the space charge region cannot be neglected. Other related properties of the space charge at equilibrium, e.g., surface conductivity and capacitance, can be calculated as well using the simulation results. The space charge region capacitance is obtained as the additive contribution of the individual space charge elements connected in series, each having a capacitance of $C_K = q_K/E_K \Delta x$ where q_K is the charge in element K . The surface conductivity may be deduced by considering

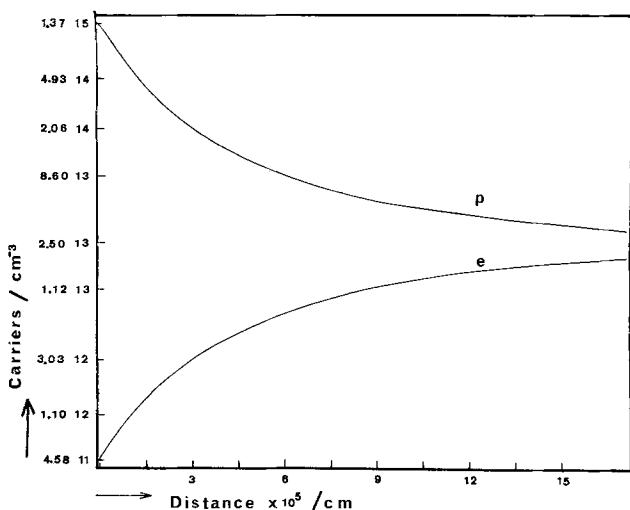


Fig. 2. Carrier concentration at equilibrium for intrinsic Ge. $V_s = 100$ mV; $p^0 = n^0 = 2.5 \times 10^{13}$ cm $^{-3}$; $\epsilon_r = 16$ esu.

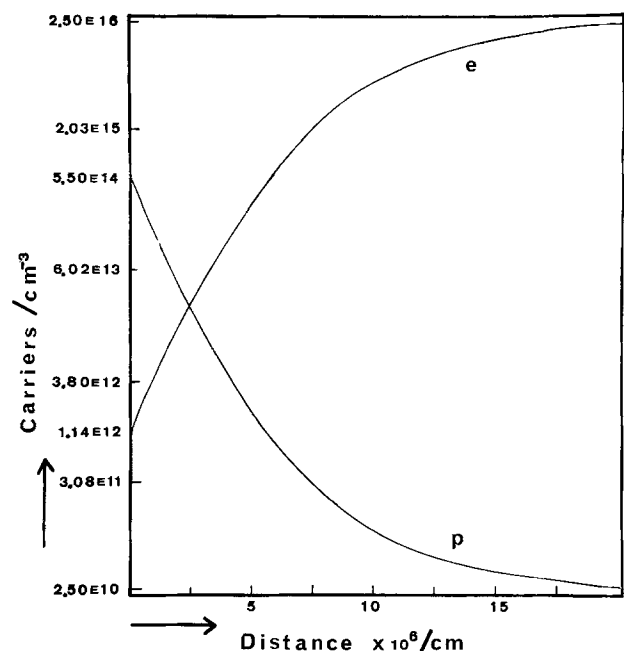


Fig. 3. Carrier concentration at equilibrium for n-type Ge. $V_s = 250$ mV; $n^0 = 2.5 \times 10^{16}$; $p^0 = 2.5 \times 10^{10}$; $\epsilon_r = 16$ esu.

the elements as representing resistors connected in parallel, each with a conductivity of $e\Delta x(U_n n_K + U_p p_K)$.

The photopotential effect.—Assume the initially biased semiconductor (now at open circuit) is illuminated with a constant light intensity. We now calculate the open-circuit, steady-state photopotential using an iterative procedure similar to that just described. A treatment of the time-dependent relaxation of carrier concentration, field, and surface potential under closed-circuit conditions is treated in the next paper in this series (11). The process at open circuit is a coulstatic one; charge in the semiconductor is conserved and the effect of light is simply to rearrange the concentration and field profiles within the semiconductor. (The same would hold true even when a faradaic current flows, if the number of holes crossing the interface is balanced by electrons extracted at the semiconductor ohmic contact or vice versa.) Consider an n-type semiconductor biased at a positive potential with respect to the solution. Under illumination the photogenerated holes will accumulate at the semiconductor surface and the electrons will move to the space charge region/semicon-

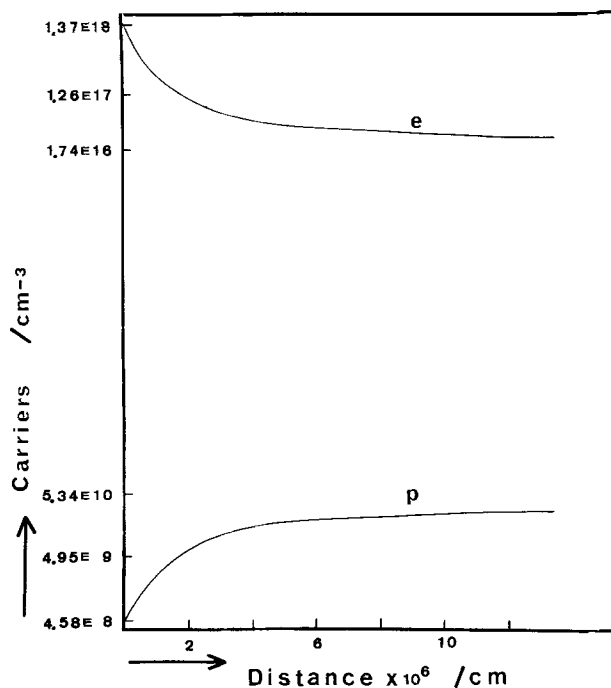


Fig. 4. Carrier concentration at equilibrium for n-type Ge (sample as in Fig. 2). $V_s = -100$ mV.

ductor bulk boundary. The dimensions of the space charge region will change to accommodate these shifts in carrier concentration. The total charge, and hence the surface field, will remain constant, so that the semiconductor space charge region can be compared to a capacitor with a given charge which undergoes a decrease in its width resulting in an increase in capacitance and thus a decrease in the voltage drop across it under illumination. The steady state is characterized by the value of E_s , the surface field, known from the initial condition (Boltzmann distribution), and by the "minority injection level," here, the hole concentration immediately beyond the space charge region, which is directly proportional to illumination intensity. Analytical procedures exist for the rigorous determination of the injection level of minority carriers (here, holes) (12). For Ge, one can assume the existence of a diffusion layer, L_p , through which excess holes diffuse into the bulk (where $L_p = \sqrt{D_p \tau_p}$). L_p is much wider than the space charge region thickness (L_1) and if light is absorbed mainly in the space charge region, the expression obtained for the flux of holes at the space charge region/bulk boundary ($x = L_1$) is (3)

$$j_p(L_1) = D_p(\partial(\Delta p)/\partial x)_{x=L_1} = D_p(p_{L_1} - p^0)/L_p \quad [12]$$

Table II. Comparison of the simulated electrical properties of a large bandgap semiconductor electrode (n-type TiO $_2$) and the electrostatic approximation of the depletion layer*

| Simulated | | | | Depletion layer approximation | |
|-----------------------------------------|---------------------------------------|----------------------------------|------------|---------------------------------------|------------------|
| Q_s C/cm 2 ($\times 10^7$) | E_s V/cm ($\times 10^{-4}$) | L_1 cm ($\times 10^6$) | V_s V | L_1^{**} cm ($\times 10^6$) | V_s^{***} V |
| 1.485 | 1.677 | 1.56 | 0.100 | 0.928 | 0.078 |
| 2.243 | 2.533 | 1.92 | 0.200 | 1.40 | 0.178 |
| 3.249 | 3.670 | 2.36 | 0.393 | 2.03 | 0.373 |
| 4.001 | 4.519 | 2.76 | 0.585 | 2.50 | 0.565 |
| 4.675 | 5.774 | 3.16 | 0.777 | 2.89 | 0.755 |
| 5.166 | 5.835 | 3.36 | 0.963 | 3.23 | 0.943 |
| 5.752 | 6.496 | 3.76 | 1.188 | 3.595 | 1.168 |
| 6.271 | 7.083 | 4.00 | 1.408 | 3.91 | 1.388 |

* Assumed to consist of only immobile donors; $N_D = 10^{17}$ cm $^{-3}$; $\epsilon_r = 100$ esu.
 ** $L_1 = Q_s/l \cdot N_D$ (depletion layer width).
 *** $V_s = E_s/2L_1$ (E_s , surface field; V_s , surface potential).

From Eq. [3] this same flux is given by

$$j_p(L_1) = -I_0(1 - e^{-aL_1}) + \int_0^{L_1} R(x) dx \quad [13]$$

Equations [12] and [13] allow the assignment of an initial value to p_{L_1} (assuming at first no recombination in the space charge region) which is modified during the simulation due to the recombination term, using the given values of I_0 , a , and the semiconductor properties ($D_p\tau_p$). The equivalent expression for the electrons is

$$n_{L_1} = n^0 + (p_{L_1} - p^0) \quad [14]$$

because in this region electroneutrality essentially holds (13). In more complicated cases, when L_p and L_1 are comparable in magnitude, light is absorbed outside the space charge region as well and linearization of the diffusion layer is unjustified. In this case a simulation involving a fuller treatment of the diffusion layer can be undertaken to find the injection level.

p_{L_1} and n_{L_1} serve as boundary conditions for the recursion formula between the elements, this time taken from the space charge region/semiconductor bulk boundary to the surface which at the steady state, according to Eq. [3] and [4] and Table I, is given by

$$p_K = \frac{L(K) - \Sigma R(K) + [0.5 U_p E_{K+1} + (D_p/\Delta x)] \cdot p_{K+1}}{(D_p/\Delta x) - 0.5 U_p E_{K+1}} \quad [15a]$$

$$n_K = \frac{L(K) - \Sigma R(K) - [0.5 U_n E_{K+1} - (D_n/\Delta x)] \cdot n_{K+1}}{(D_n/\Delta x) - 0.5 U_n E_{K+1}} \quad [15b]$$

where

$$L(K) = I_0(1 - e^{-a(K-1/2)\Delta x}) \quad [\text{cm}^{-2}\text{sec}^{-1}] \quad [16]$$

$$\Sigma R(K) = \sum_{K=1}^K \left(\frac{p_K - p_K^{\text{eq}}}{\tau_p} \frac{n_K}{n^0} \Delta x \right) \quad [\text{cm}^{-2}\text{sec}^{-1}] \quad [17]$$

The electric fields are calculated with Eq. [11], this time proceeding from the surface to the bulk because the surface field is known.

Thus, starting with the semiconductor in the dark at a surface potential V_s , the condition under illumination is simulated by repetitively using Eq. [12]-[17] until three new constant arrays (holes, electrons, and electric field) are obtained. A numerical integration over the fields yields a new surface potential, V_s' , where the photopotential, ΔV , is $V_s - V_s'$.

Results

The simulated distribution of carriers with and without illumination is shown in Fig. 5; Fig. 6 compares the electric fields under these conditions. The dependence of the photopotential on the equilibrium surface potential which exists before illumination obtained by the simulation compared to the calculation method of Johnson (4) is given in Fig. 7 and the relation between the photopotential and the illumination intensity obtained by these two methods is shown in Fig. 8. Johnson's method of obtaining the photopotential usually uses the assumption that the Boltzmann distribution and the same analytical expression relating the potential and the field for the semiconductor holds both in the dark and as well as in the light (3, 4). This assumption was checked by the digital simulation and indeed we find that Eq. [18] and [19] hold

$$p_s' \simeq p_{L_1}' \exp(eV_s'/kT) \quad [18]$$

$$n_s' \simeq n^0 \exp(eV_s'/kT) \quad (n_{L_1}' \simeq n^0) \quad [19]$$

where the primed quantities denote values under illumination. This assumption applies, as has been pointed out previously (12), because there is fast trans-

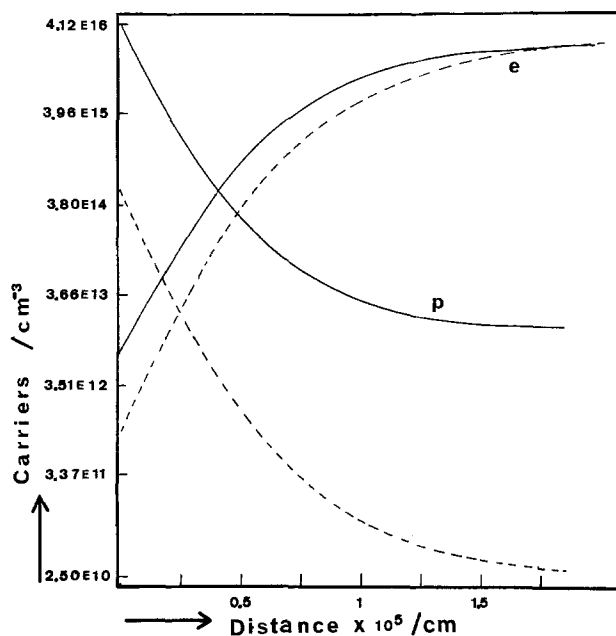


Fig. 5. Carrier concentration at steady state with constant illumination for n-type Ge (sample as in Fig. 3). $I_0 = 10^{16}$ photons/cm²-sec, V_s (dark) = 250 mV. The dashed lines show the equilibrium concentration in the dark.

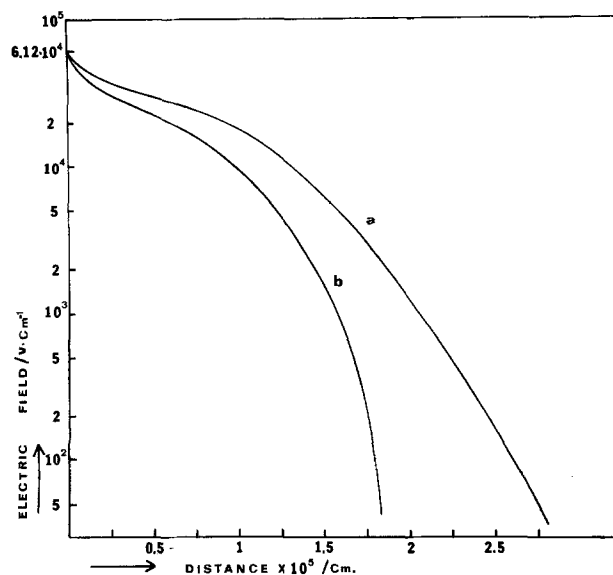


Fig. 6. Electric fields for n-type Ge (sample as in Fig. 3): (a) in the dark and (b) under constant illumination, $I_0 = 10^{16}$ photons/cm²-sec. V_s (dark) = 400 mV.

port within the semiconductor phase. Thus only a very slight imbalance between the diffusional and the migrational fluxes (compared to their absolute magnitude) has to exist to provide the nonequilibrium flux which corresponds to moderate illumination. Hence, in practice, even under illumination, the carriers and electrical field will be distributed in such a way that $u_i n_i E_i \simeq D_i (\partial n_i / \partial x)$, which leads to the same functional relation as in the dark.

Acknowledgment

The support of this research by the National Science Foundation (MPS74-23210) is gratefully acknowledged.

Manuscript submitted Feb. 3, 1976; revised manuscript received Feb. 7, 1976.

Any discussion of this paper will appear in a Discussion Section to be published in the June 1977 JOURNAL. All discussions for the June 1977 Discussion Section should be submitted by Feb. 1, 1977.

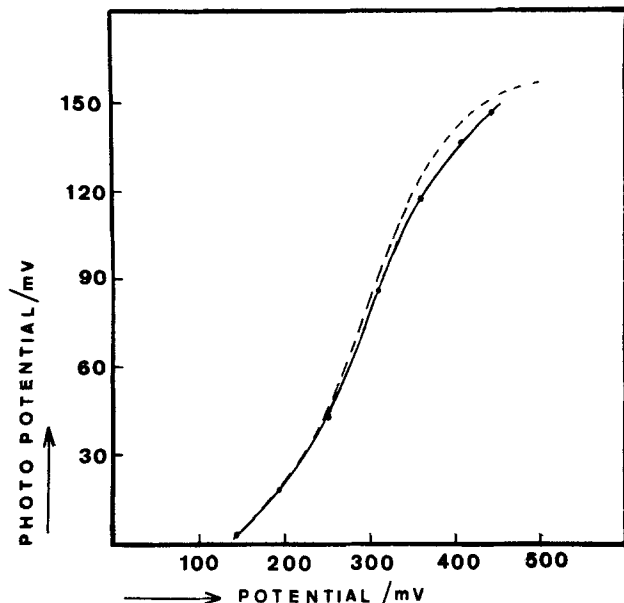


Fig. 7. The dependence of the photopotential for n-type Ge (sample as in Fig. 3) on dark surface potential V_s ; $I_0 = 10^{16}$ photons/cm²-sec. Dashed line, calculated according to Johnson's method (4) assuming $pL_1 = 1.3 \times 10^{13}$ cm⁻³ (see text).

Publication costs of this article were assisted by The University of Texas at Austin.

REFERENCES

1. D. Laser and A. J. Bard, *This Journal*, **123**, 1828 (1976).
2. M. D. Archer, *J. Appl. Electrochem.*, **5**, 17 (1975).
3. C. G. B. Garrett and W. H. Brattain, *Phys. Rev.*, **99**, 376 (1955).
4. E. O. Johnson, *ibid.*, **111**, 153 (1958).
5. S. W. Feldberg, in "Electroanalytical Chemistry,"

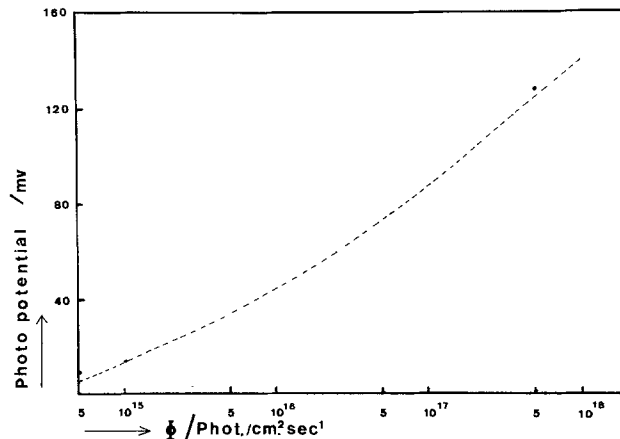


Fig. 8. Dependence of photopotential for n-type Ge (sample as in Fig. 2) on illumination intensity. V_s (dark) = 250 mV. Points are simulations and the dashed line was calculated by Johnson's method (4) assuming that the injection level was proportional to the light intensity and was 1.3×10^{13} cm⁻³ at an illumination intensity of 10^{16} photons/cm²-sec.

- Vol. 3, A. J. Bard, Editor, chap. 4, Marcel Dekker, Inc., New York (1969).
6. H. Gerischer, *This Journal*, **113**, 1174 (1966).
7. V. A. Myamlin and Yu. V. Pleskov, "Electrochemistry of Semiconductors," pp. 30-50, Plenum Press, New York (1967).
8. A. Many, Y. Goldstein, and N. B. Grover, "Semiconductor Surfaces," chap. 4, John Wiley & Sons, Inc., New York (1965).
9. V. A. Myamlin and Yu. V. Pleskov, *op. cit.*, p. 18.
10. *Ibid.*, p. 55.
11. D. Laser and A. J. Bard, *This Journal*, **123**, 1837 (1976).
12. A. Rothwarf and K. W. Böer, "Progress in Solid State Chemistry," Vol. 10, p. 71, Pergamon Press, Oxford (1975).
13. V. A. Myamlin and Yu. V. Pleskov, *op. cit.*, p. 182.

Semiconductor Electrodes

IX. Digital Simulation of the Relaxation of Photogenerated Free Carriers and Photocurrents

Daniel Laser and Allen J. Bard*

Department of Chemistry, The University of Texas at Austin, Austin, Texas 78712

ABSTRACT

A digital simulation of the photoprocess at a semiconductor electrode is described. The simulation model accounts for photogeneration, recombination, and transport of excess free carriers within the semiconductor phase. The origin of the photopotential in the absence of faradaic current is elucidated. Quantitative current efficiency-potential curves for the photocurrents under a variety of conditions are calculated for n-type TiO₂ and these are compared to experimental results.

In previous papers in this series we have introduced the use of digital simulation methods for the treatment of semiconductor electrodes. In Ref. (1) the relaxation of free carriers following charge injection, with and without surface states, was described. In Ref. (2) a method of deriving the semiconductor electrode characteristics, equilibrium or steady state, at open circuit in the dark or under constant illumination, was presented. When a semiconductor electrode at equilibrium and in contact with solution is illuminated, a certain

time elapses before the photoeffects are observed. During this time a redistribution of free carriers and charges in the electric field in the space charge region occurs. [When the semiconductor electrode/solution interface is blocked to charge transfer, the new distribution of free carriers in the space charge region under illumination will cause a change in the potential of the electrode (the photopotential effect).] Frequently, illumination of the electrode is accompanied by charge transfer to solution species and this gives rise to a photocurrent. For example, irradiation of n-type TiO₂ with light of energy larger than the bandgap energy will result in the oxidation of water (3, 4), while

* Electrochemical Society Active Member.

Key words: semiconductors, digital simulation, photoelectrochemistry, photogalvanic cells.